

Synergistic Photoredox/Palladium Catalysis Enables Enantioconvergent Cross-Electrophile Esterification with CO₂

Bihai Ye,^{[a][b]} Lei Su,^{[a][b]} Kaiting Zheng,^{[a][b]} Shen Gao^{[a][b]}, and Jiawang Liu^{*[a][b]}

[a] Frontiers Science Center for Transformative Molecules, Shanghai Key Laboratory for Molecular Engineering of Chiral Drugs, School of Chemistry and Chemical Engineering, Shanghai Jiao Tong University, Shanghai, 200240 China

[b] Zhangjiang Institute for Advanced Study, Shanghai Jiao Tong University, Shanghai, 201203 China

E-mail: liujw2020@sjtu.edu.cn

Abstract: Herein, we presented a synergistic catalytic system that utilizes 4CzIPN and (R)-L1/Pd(acac)₂ as catalysts for an efficient and enantioconvergent synthesis of axially chiral esters from racemic heterobiaryl bromides and alkyl bromides with CO₂ under mild conditions. A wide range of axially chiral esters, featuring various functional groups, were obtained through this novel methodology in good to high yields with excellent enantioselectivities. Detailed mechanistic studies unveiled that the ratio of 4CzIPN/[Pd/(R)-L1] significantly influences the chemo- and enantioselectivity of the reaction. Kinetic studies and control experiments supported the proposed mechanism involving cascade asymmetric carboxylation followed by S_N2 substitution. Achieving high enantioselectivities relies not only on the choice of synergistic metallaphotoredox catalysts but also on the utilization of alkyl bromides, which trap the generated chiral carboxylic anions in situ, preventing their immediate racemization.

Introduction

Synergistic photoredox/transition metal catalysis, commonly referred to as metallaphotoredox, has emerged as a reliable strategy for designing and developing new transformations under mild conditions.^[1] Compared to single catalytic systems, metallaphotoredox catalysis combines the unrivaled capability of transition metal catalysis for bond formation with the broad utility of photoinduced electron- or energy-transfer processes, which facilitates the success of challenging chemical transformations.^[2] Among the various established metallaphotoredox catalytic systems, the reductive cross-coupling reactions have been extensively studied that afford a straightforward and modular approach to access valuable complex targets from two readily available electrophiles.^[3] In contrast to traditional reductive cross coupling reactions, this photoredox-assisted reductive strategy not only avoids the use of superstoichiometric metal reductants (e.g., Zn, Mn, ZnEt₂), but also improves the catalyst's performance as well as enables precise control over multiple selectivities via modulation of two independent catalytic cycles. Although significant progresses have been achieved in this realm, metallaphotoredox catalyzed reactions employing CO₂ as one of the electrophiles to synthesize carboxylic acids via C-C bond formation,^[4] especially in an enantioselective manner, remains in its infancy (Figure 1a).

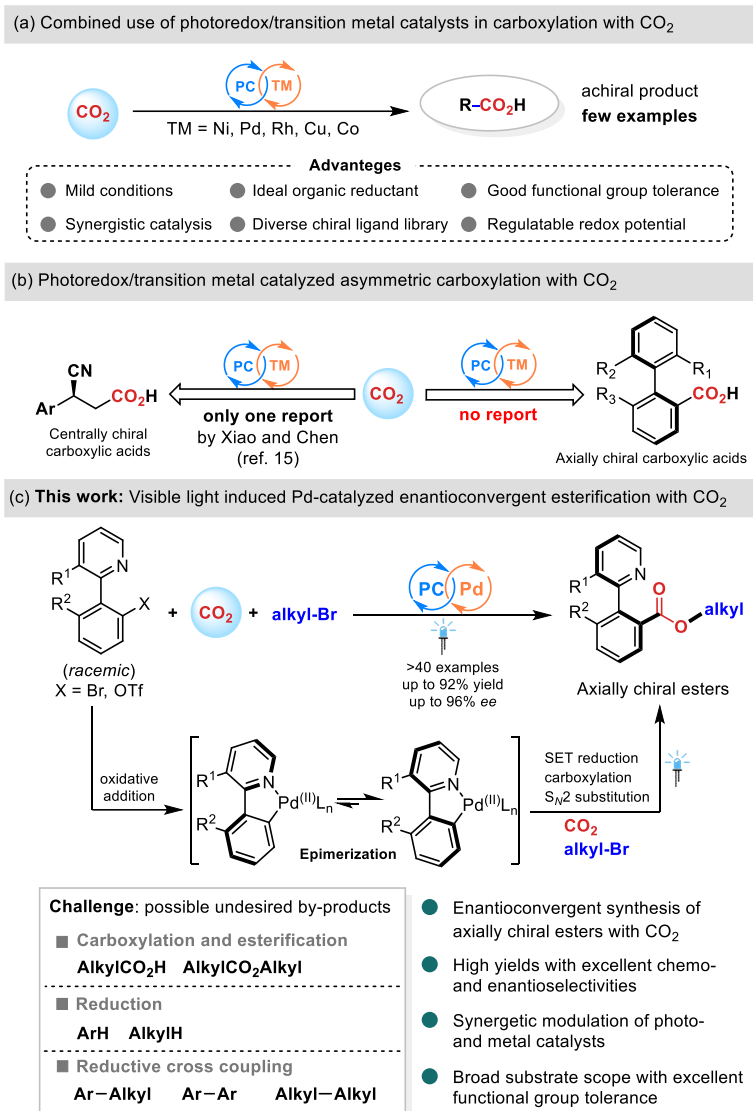


Figure 1. Transition metal-catalyzed asymmetric C–C bond formation with CO₂.

Carbon dioxide (CO₂), known as a non-toxic, abundant, and sustainable carbon feedstock, has attracted substantial attention from the synthetic community. Over the past few decades, extensive efforts have been devoted to the utilization of CO₂ as a C1 source to produce fine chemicals, and significant achievements were made.^[5] Nevertheless, the catalytic asymmetric transformation of CO₂, particularly through the formation of C–C bond to synthesize enantioenriched carboxylic acids or their derivatives, remains an extraordinary challenge.^[6] Due to inherent kinetic inertness and thermodynamic stability of CO₂, its transformation often necessitates the provision of considerable energy that leads to the use of harsher reaction conditions than desired. Another challenging issue might be the relatively weak coordination ability of CO₂ towards catalytic metal centers. Consequently, only a handful of effective catalytic systems for asymmetric carboxylation with CO₂ have been developed so far, albeit these methods require the use of an excess amount of metallic reagents, silanes, boron reagents or electrochemical conditions to sustain the catalytic cycle.^[7] Of particularly note, most established methodologies focus on carboxylic acids with central chirality, yet the synthesis of axially chiral carboxylic acids and their derivatives with CO₂ are still underdeveloped due to the lack of a suitable catalytic system.^[8] On the other hand, the axially chiral carboxylic acids and their derivatives usually serve as highly efficient

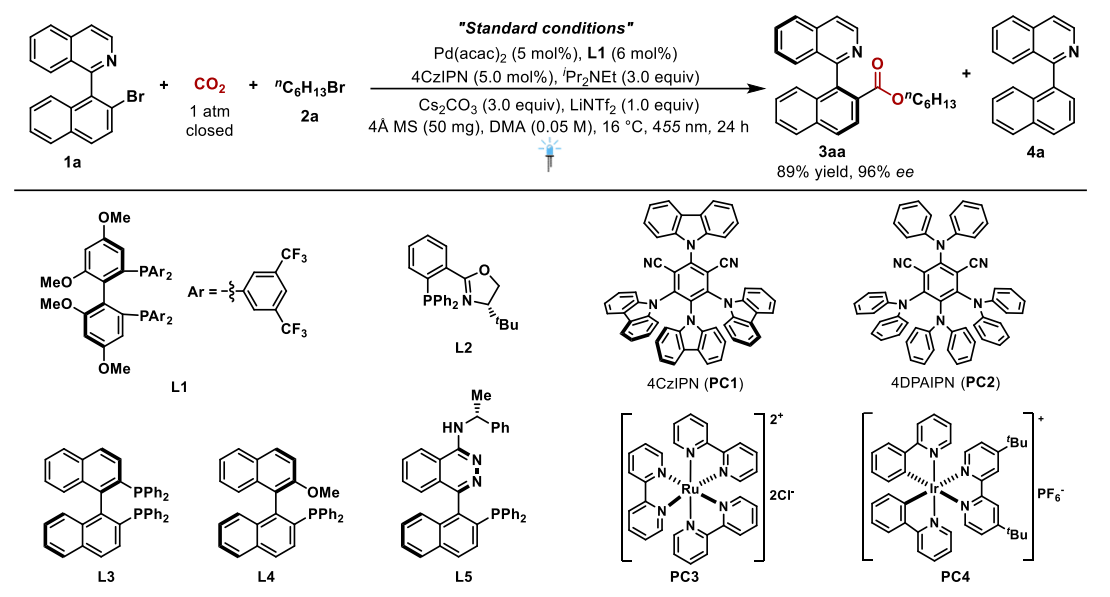
catalysts or ligands in diverse asymmetric transformations.^[9] Therefore, the development of efficient and novel catalytic systems to realize asymmetric carboxylation with CO₂, especially the synthesis of axially chiral carboxylic acids is still in high demand.^[10]

Considering that there are numerous combinations of dual photoredox/transition metal catalysts by varying ligand, photocatalyst, or organic reductant, it offered the prospect of achieving asymmetric carboxylation with CO₂, so we decided to explore the feasibility for employing such a catalytic system. The pioneering work of metallaphotoredox catalyzed CO₂ transformation were reported by Murakami and co-workers in 2016, which combined the use of Cu and ketone as catalysts for carboxylation of allylic C-H bonds with CO₂ under UV-light.^[11] Subsequently, visible-light-driven metallaphotoredox catalysis was established by the use of Rh,^[12] Ni,^[13] Pd,^[14] Co^[15] and Cu^[4c] with matched photocatalysts that has enabled direct carboxylation of CO₂ under mild conditions with various organic substrates, such as alkenes, organohalides, alkynes etc. (Figure 1a). Nevertheless, the asymmetric version of the related transformation was scarcely investigated until very recently, where the Xiao and Chen group developed an effective metallaphotoredox-enabled asymmetric difunctionalization of alkenes with CO₂ via an alkene radical anion strategy, affording a series of chiral carboxylic acids with the chiral center at the β-position (Figure 1b, left).^[16] To the best of our knowledge, the enantioselective transformation of CO₂ through photoredox/transition metal catalysts to produce axially chiral carboxylic acids or esters has not yet been reported (Figure 1b, right).

Herein, we present our recent results on the dual photoredox/Pd catalyzed enantioconvergent cross-electrophile esterification of racemic heterobiaryl (pseudo)halides and alkyl bromides with CO₂ under visible light irradiation, yielding a series of axially chiral esters with excellent enantioselectivity (Figure 1c). Based on previous reports,^[17] we expected the chelated-cyclopalladium intermediate, generated by oxidative addition of palladium to racemic heterobiaryl (pseudo)halides, to undergo epimerization via a dynamic kinetic asymmetric transformation (DyKAT) to accomplish deracemization of the substrate (Figure 1c). Notably, in our initial trials using racemic heterobiaryl (pseudo)halides with CO₂, we noted that the enantiomeric excess of the obtained axially chiral carboxylic acids was significantly lower than that of the esterified product in situ in the presence of alkyl bromides (Table 1, entries 1 and 6). However, incorporating alkyl bromide as the third electrophile may increase the complexity of achieving high chemoselectivity, considering potential competing carboxylation, reduction, and reductive cross-electrophile coupling of organobromides. Fortunately, by applying an appropriate combination of a ligated chiral palladium catalyst and a matched photocatalyst with diisopropylethylamine (DIPEA) as the final reductant, the side-products could be inhibited to a very low level, thus realizing the first enantioconvergent synthesis of axially chiral esters under very mild conditions.

Results and Discussion

We commenced our investigation into the photoredox/palladium catalyzed cross-electrophile esterification by using racemic 1-(2-bromonaphthalen-1-yl)isoquinoline (**1a**), 1-bromohexane (**2a**), and CO₂ as the reaction partners under typical conditions for metallaphotoredox catalyzed reactions [4CzIPN as a photocatalyst, diisopropylethylamine (DIPEA) as a reductant, Pd salt as a metal catalyst, and blue LEDs, as shown in Table 1]. We began by evaluating the effect of chiral ligands on the reaction by using Pd(acac)₂ as the catalyst and it was found that the ligand had a significant influence on the reactivity (Table 1, entries 1-5). The axially chiral bisphosphine ligand **L1** gave the best result, affording the axially

Table 1. Optimization of the reaction conditions. ^[a]

entry	Variations from the standard conditions	Yield of 3aa (%) ^[a]	ee of 3aa (%) ^[a]	entry	Variations from the standard conditions	Yield of 3aa (%) ^[a]	ee of 3aa (%) ^[a]
1	none	89	96	10	HEH instead of DIPEA	34	92
2	L2 instead of L1	0	--	11	LiOTf instead of LiNTf ₂	45	56
3	L3 instead of L1	0	--	12	LiCl instead of LiNTf ₂	40	62
4	L4 instead of L1	28	0	13	NaN Tf ₂ instead of LiNTf ₂	83	92
5	L5 instead of L1	29	42	14	w/o LiNTf ₂	79	82
6 ^[b]	w/o ⁿ C ₆ H ₁₃ Br (2a)	82	6	15	w/o 4 Å MS	74	96
7	PC2 instead of PC1	72	60	16	w/o Cs ₂ CO ₃	32	93
8	PC3 instead of PC1	0	--	17	N ₂ instead of CO ₂	0	--
9	PC4 instead of PC1	62	84	18	no Pd/L1, or no PC1 or no light	0	--

[a] Standard conditions: **1a** (0.1 mmol, 1.0 equiv.), **2a** (0.3 mmol), CO₂ (1.0 atm, closed), Pd(acac)₂ (5.0 mol%), L1 (6.0 mol%), 4CzIPN (5.0 mol%), DIPEA (3.0 equiv.), Cs₂CO₃ (3.0 equiv.), LiNTf₂ (1.0 equiv.), 4 Å MS (50 mg) in DMA (2.0 mL), blue LED (455 nm) at 16 °C for 24 h. The yields were isolated yields for all products by column chromatography, and the ee (enantiomer excess) was determined by HPLC using a chiral column. [b] After 24 hours, **2a** was added into the reaction mixture and stirred for 4 hours. HEH = diethyl 2,6-dimethyl-1,4-dihydropyridine-3,5-dicarboxylate, DMA = *N,N*-dimethylacetamide, DIPEA = diisopropylethylamine.

chiral ester **3aa** in 89% yield with 96% ee (standard conditions, Table 1, entry 1). Notably, under the standard conditions, the side reactions could be suppressed and only the hydrodehalogenated byproduct **4a** was observed in less than 10%, which contrasts with previous reports of nickel/photoredox catalysis^[18]. To demonstrate the necessity of alkyl bromide (**2a**), we conducted a control experiment in the absence of **2a** under the same conditions. Surprisingly, although the product **3aa** could be obtained in 82% yield after esterification with 1-bromohexane (**2a**), the enantioselectivity dramatically decrease to 6% ee (Table 1, entry 6). These results suggested that the carboxylation process proceeded efficiently in high enantioselectivity, however the resulted carboxylic anion might undergo racemization under the standard

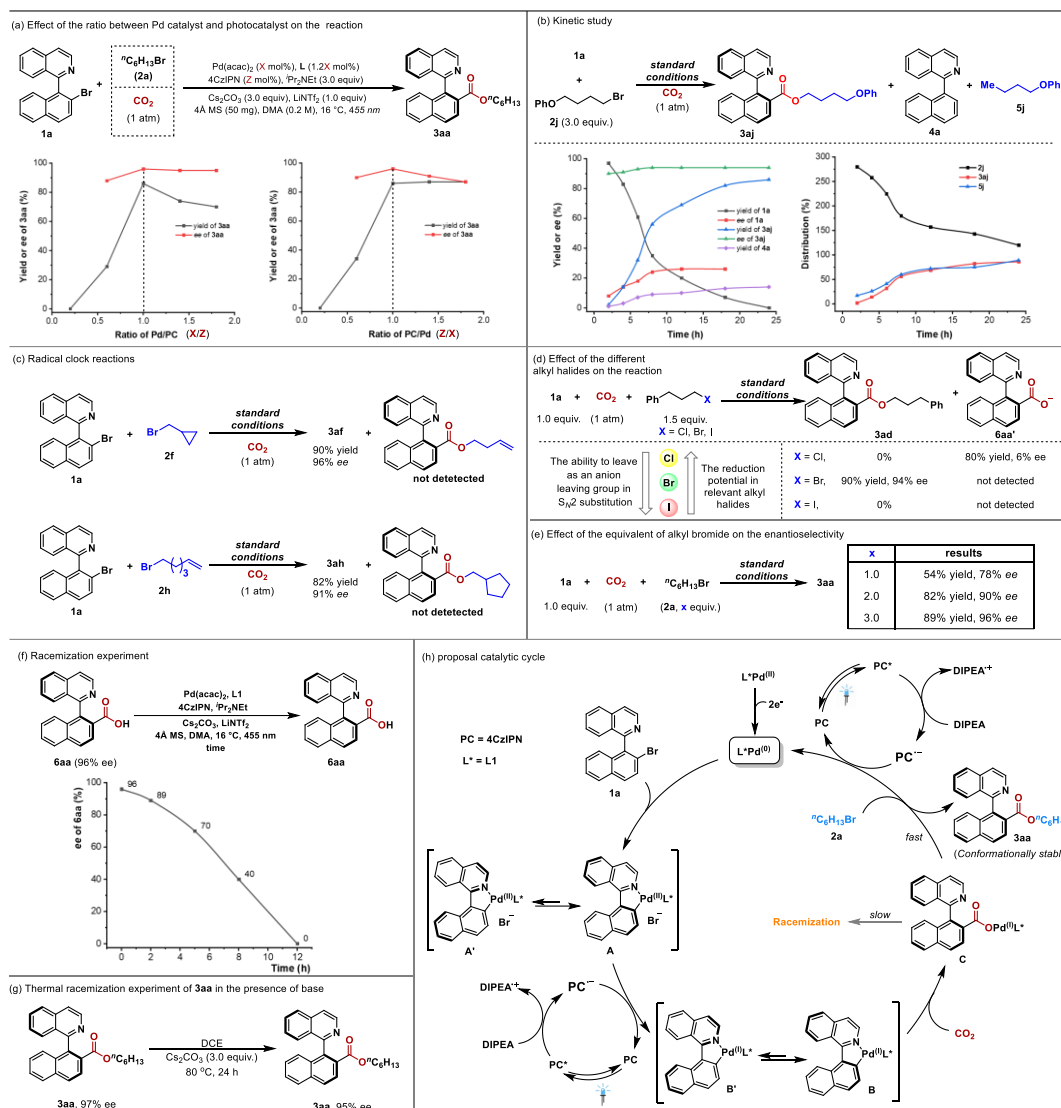
conditions. Different photocatalysts, such as 4DPAIPN (**PC2**), Ru(bpy)₃Cl₂ (**PC3**), and Ir(ppy)₂(dtbpy)PF₆ (**PC4**), were evaluated, but lower yields and enantioselectivities were obtained in all cases (Table 1, entries 7-9). Using Hantzsch ester (HEH) as the reductant instead of DIPEA only provided the desired product **3aa** in 32% yield with 92% ee due to the incomplete conversion of **1a** (Table 1, entry 10), which indicated that SET reduction of the Pd^(II) intermediate might be a slow step. Other additives with different cations or anions, including LiOTf, LiCl, and NaNTf₂, were also introduced into the reaction instead of LiNTf₂. The former two lithium salts gave **3aa** in moderate yields and enantioselectivities, accompanied by a large amount of **4a** (Table 1, entries 11 and 12), and the latter (NaNTf₂) had a slight influence on the reaction (Table 1, entry 13). These results implied that the NTf₂ anion has a significant impact on the reaction performance, which was supported by the result in the absence of LiNTf₂ (Table 1, entry 14). This is probably attributed to the weak coordination of the NTf₂ anion, facilitating the generation and epimerization of the cyclopalladium intermediate. Moreover, 4Å molecular sieves could promote the yield by suppressing competitive reductive protonation (Table 1, entry 15). Additionally, the role of Cs₂CO₃ as a base rather than a CO₂ surrogate was illustrated by the results as there was no desired product detected under nitrogen (Table 1, entries 16 and 17). Finally, we carried out a series of controlled experiments to indicate that the metal, ligand, photocatalyst **PC1**, and light are all necessary for the cross-electrophile esterification under standard conditions (Table 1, entry 18).

With the optimized conditions in hand, we began to investigate the substrate scope for this asymmetric three-component esterification, which utilizes CO₂ to synthesize various axially chiral esters. First, the scope of alkyl bromides was studied under the standard conditions and the results were summarized in Table 2. The reaction appears to be compatible with various types of alkyl bromides (**2a-2ee**), consistently affording the corresponding axially chiral esters in high yields (80-92%) with excellent enantioselectivities (90-96% ee). In the presence of an array of alkyl bromides with different chain lengths, the cascade carboxylation and substitution steps underwent smoothly, delivering the corresponding chiral esters **3ab-3ae** in 87-91% yields with 92-96% ee. Moreover, alkyl bromides with different functional groups such as cyclopropane, alkene, methoxy, phenoxy, ester, cyano, and trifluoromethyl, also reacted efficiently, affording the desired esters **3af-3an** in high yields with excellent enantioselectivity. The reaction with alkyl bromides bearing alkyl chloride and fluoride that might influence chemoselectivity gave the desired products **3ao** and **3ap** in 91-92% yield with the same 96% ee. The functional groups of methylsulfonyl (**3aq**), phosphonate (**3ar**), amide (**3at**), and ketone (**3ax**) were well-tolerated in the catalysis. Besides, this chiral ester synthesis method could provide diesters (**3as, 3au-3aw**) in 86-90% yield with 94-95% ee. Notably, the substrates with a heteroarene such as thiophene, furan, benzofuran, and isoquinoline also worked well under the visible light conditions and accomplished the corresponding products **3ay-3abb** in 85-89% yield with 93-96% ee. Finally, the substrates containing drug fragments such as Isoxepac, Ibuprofen, and Diacetone-*D*-glucose, participated in this transformation efficiently to provide **3acc-3aee**.

Next, a survey of various heterobiaryl bromides or triflates was performed in the photoredox/Pd-catalyzed cross-electrophile esterification with CO₂ by using 1-bromo-4-methoxybutane (**2i**) as the third coupling partner. As shown in Table 2, substitutes such as methoxy, methyl, fluoride, and phenyl group on the 4th and 5th positions of the naphthyl ring did not affect the reaction and provided the corresponding products (**3bi-3fi**) in 80-88% yields with 90-94% ee. Notably, the reaction scope is not limited to the naphthyl scaffold as the reaction employing bulky bromobenzene **1g** also proceeded with a high level of asymmetric induction (**3gi**). To our delight, the heteroaryl bromide substrates derived from quinazoline ring also

To gain more insight into the synergistic photoredox and palladium catalytic system, a series of control experiments were performed (Scheme 1). Firstly, the impact of the ratio between the palladium catalyst [Pd(acac)₂/L1] and photocatalyst (4CzIPN) on the reaction was investigated by varying one of the catalyst loadings. Interestingly, the yield and ee of **3aa** reached the highest peak value simultaneously when the quantities of the palladium catalyst and photocatalyst were equal, suggesting that the synergy was optimal at this ratio (Scheme 1a). Then, the kinetic study was conducted under the standard conditions. Along with the consumption of **1a**, the yield of **3aj** increased gradually, and the ee of **3aj** was almost constant (>90%) until the end of the reaction. The observed low ee of recovered **1a** indicated that this process might occur in a non-ideal kinetic manner in the presence of Pd/L1 (Scheme 1a, left). In the same kinetic investigation, we also observed the generation of **5j** in a considerable amount, from alkyl bromide **2j**, via a hydrodehalogenated process (Scheme 1a, right). The results of the radical clock experiments demonstrated that the formation of esters with alkyl bromides does not involve a radical species (Scheme 1c). Interestingly, in the reactions using (3-chloropropyl)benzene or (3-iodopropyl)benzene instead of (3-bromopropyl)benzene (**2d**), there was no desired ester product **3ad** detected (Scheme 1d). In the case of (3-chloropropyl)benzene, carboxylation of **1a** with CO₂ occurred smoothly, however due to the poor leaving ability of chlorine as an anion, the subsequent substitution reaction did not take place. Hence, the carboxylic anion **6aa'** was detected and isolated in 80% yield and 6% ee. In the case of (3-iodopropyl)benzene, carboxylation did not proceed at all, which was likely owing to the easier reduction of alkyl iodide that disrupted the desired reaction (Scheme 1d). All the above experimental results supported that the esterification process most likely proceeded through S_N2 substitution between the carboxylic acid anion and alkyl bromide. To investigate the influence of S_N2 substitution between the carboxylic anion and alkyl bromide on enantioselectivity, a set of experiments was carried out by using different equivalents of **3a** (Scheme 1e). As expected, the yield and ee of **3aa** were both promoted by increasing the concentration of **2a**, which was consistent with the results (Table 1, entry 6 and Scheme 1b, right). Furthermore, the study on the conformational stability of carboxylic anion demonstrated that under the standard conditions, the generated carboxylic acid **6aa** would undergo racemization over time (Scheme 1f). Fortunately, after esterification in situ with alkyl bromide **2a**, the compound **3aa** was thermally stable even with heating at 80 °C (Scheme 1g).

Based on our mechanistic studies and literature reports,^{[14][19]} a plausible catalytic cycle was proposed (Scheme 1h). First, the Pd^{II}/L1 complex was reduced to Pd⁰/L1,^[14a-c, 20] followed by coordination and oxidative addition to racemic heterobiaryl bromide **1a** to form cyclopalladium species **A** and **A'**, which would undergo subsequent epimerization to start the deracemization process of the substrate induced by the chiral ligand L1.^[17] According to previous studies, cyclopalladium **A** or **A'** do not undergo carboxylation with CO₂ due to a high energy barrier.^{[19][21]} Therefore, in this case, they would undergo single electron induction to ArPd^IL* species **B** and **B'** by PC^{•-} (4CzIPN^{•-}), which was generated from the excited photocatalyst and DIPEA under visible light. During this single electron induction process, epimerization may continue to proceed to realize a dynamic kinetic asymmetric transformation. Upon generation of ArPd^IL* (**B** and **B'**), coordination and migratory insertion with CO₂ took place to afford carboxylic Pd^I intermediate **C** since the ArPd^IL* complex was reported as the active species in Pd-catalyzed reductive carboxylation of aryl halides with CO₂.^[19] In our catalytic system, palladium(I) carboxylate **C** would be trapped in situ by alkyl bromide **2a** to afford ester **3aa** immediately, otherwise it would undergo racemization and the enantioselectivity would be eroded gradually. Meanwhile, the released Pd^IL* species was reduced to Pd⁰L* to close the whole catalytic cycle.



Scheme 1. Mechanistic study.

Conclusion

In conclusion, we have established an efficient dual photoredox/transition metal catalytic system by combined use of 4CzIPN and (*R*)-L1/Pd(acac)₂, facilitating the enantioconvergent cross-electrophile esterification of racemic heterobiaryl bromides and alkyl bromides with CO₂ for the first time. This methodology operates under mild conditions, exhibits a wide substrate scope with exceptional compatibility for various functional groups, and delivers axially chiral esters in good to high yields with excellent enantioselectivity. Mechanistic studies illustrate the importance of both the photocatalyst and palladium catalyst, as well as the crucial role of their ratio in attaining high yield and enantioselectivity. The kinetic study, radical clock reactions and control experiments with different alkyl halides (Cl, Br, I) all support the proposed mechanism wherein the reaction proceeds through cascade asymmetric carboxylation followed by S_N2 substitution rather than a radical process. Moreover, the use of an appropriate amount of alkyl bromide to trap the generated chiral carboxylic anion towards the formation of a conformationally stable ester, improved both the yield and enantioselectivity. Further application of synergistic photoredox and transition metal catalysts in asymmetric CO₂ transformations is currently ongoing in our laboratory, and the results will be reported in due course.

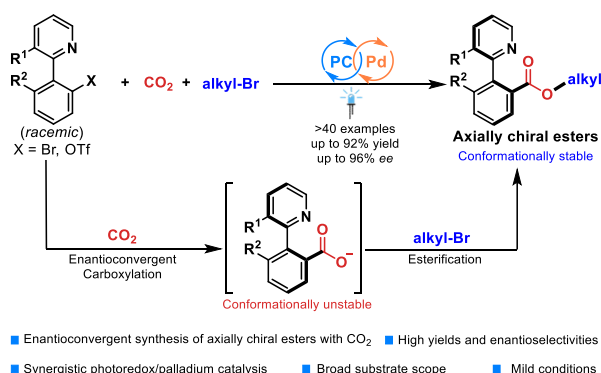
Acknowledgements

We are grateful for the financial support from the National Key R&D Program of China (2023YFA1507500), Shanghai Jiao Tong University 2030 Initiative, the Fundamental Research Funds for the Central Universities (23X010301599), National Natural Science Foundation of China (22201173, 22201175), and Shanghai Rising-Star Program (21QA1404900). We thank Prof. Chen Zhu (SJTU), Prof. Senmiao Xu (LICP), and Prof. Qing-An Chen (DICP) for helpful discussion in manuscript preparation.

Keywords: Metallaphotoredox • Carbon dioxide• Enantioconvergent carboxylation• Axially chiral esters • Three-component reaction

- (a) A. Y. Chan, I. B. Perry, N. B. Bissonnette, B. F. Buksh, G. A. Edwards, L. I. Frye, O. L. Garry, M. N. Lavagnino, B. X. Li, Y. Liang, E. Mao, A. Millet, J. V. Oakley, N. L. Reed, H. A. Sakai, C. P. Seath, D. W. C. MacMillan, *Chem. Rev.* **2022**, *122*, 1485-1542; (b) K. L. Skubi, T. R. Blum, T. P. Yoon, *Chem. Rev.* **2016**, *116*, 10035-10074; (c) A. Gualandi, M. Anselmi, F. Calogero, S. Potenti, E. Bassan, P. Ceroni, P. G. Cozzi, *Org. Biomol. Chem.* **2021**, *19*, 3527-3550; (d) M. D. Abreu, P. Belmont, E. Brachet, *Eur. J. Org. Chem.* **2020**, *10*, 1327-1378; (e) J. Zhang, M. Rueping, *Chem. Soc. Rev.* **2023**, *52*, 4099-4120.
- For selected reviews, see: (a) A. Lipp, S. O. Badir, G. A. Molander, *Angew. Chem. Int. Ed.* **2021**, *60*, 1714-1726; (b) F.-D. Lu, G.-F. He, L.-Q. Lu, W.-J. Xiao, *Green Chem.* **2021**, *23*, 5379-5393; (c) S. B. Beil, T. Q. Chen, N. E. Intermaggio, D. W. C. MacMillan, *Acc. Chem. Res.* **2022**, *55*, 3481-3494; (d) H.-H. Zhang, H. Chen, C. Zhu, S. Yu, *Sci. China Chem.* **2020**, *63*, 637-647; (e) Y. Jiang, Y. Zhang, B. C. Lee, M. J. Koh, *Angew. Chem. Int. Ed.* **2023**, *62*, e202305138. For selected examples, see: (f) Z. Zuo, D. T. Ahneman, L. Chu, J. A. Terrett, A. G. Doyle, D. W. C. MacMillan, *Science*, **2014**, *345*, 437-440; (g) J. C. Tellis, D. N. Primer, G. A. Molander, *Science*, **2014**, *345*, 433-436; (h) E. B. Corcoran, M. T. Pirnot, S. Lin, S. D. Dreher, D. A. DiRocco, I. W. Davies, S. L. Buchwald, D. W. C. MacMillan, *Science*, **2016**, *353*, 279-283; (i) E. R. Welin, C. C. Le, D. M. Arias-Rotondo, J. K. McCusker, D. W. C. MacMillan, *Science*, **2017**, *355*, 380-385; (j) Z. Dong, D. W. C. MacMillan, *Nature* **2021**, *598*, 451-456.
- (a) L. Yi, T. Ji, K.-Q. Chen, X.-Y. Chen, M. Rueping, *CCS Chem.* **2022**, *4*, 9-30; (b) S. Ye, T. Xiang, X. Li, J. Wu, *Org. Chem. Front.* **2019**, *6*, 2183-2199; (c) S. Zheng, Y. Hu, W. Yuan, *Synthesis* **2021**, *53*, 1719-1733.
- (a) G. Zhang, Y. Cheng, M. Beller, F. Chen, *Adv. Synth. Catal.* **2021**, *363*, 1583-1596; (b) B. Mao, J.-S. Wei, M. Shi, *Chem. Commun.* **2022**, *58*, 9312-9327; (c) J.-P. Yue, J.-C. Xu, H.-T. Luo, X.-W. Chen, H.-X. Song, Y. Deng, L. Yuan, J.-H. Ye, D.-G. Yu, *Nat. Catal.* **2023**, *6*, 959-968.
- For selected reviews, see: (a) P. Braunstein, D. Matt, D. Nobel, *Chem. Rev.* **1988**, *88*, 747-764; (b) T. Sakakura, J.-C. Choi, H. Yasuda, *Chem. Rev.* **2007**, *107*, 2365-2387; (c) M. Kojima, C. Bruckmeier, B. Rieger, W. A. Herrmann, F. E. Kühn, *Angew. Chem. Int. Ed.* **2011**, *50*, 8510-8537; (d) J. L. Wang, C. X. Miao, X. Y. Dou, J. Gao, L. N. He, *Curr. Org. Chem.* **2011**, *15*, 621-646; (e) M. He, Y. Sun, B. Han, *Angew. Chem. Int. Ed.* **2013**, *52*, 9620-9633; (f) L. Zhang, Z. Hou, *Chem. Sci.* **2013**, *4*, 3395-3403; (g) Q. Liu, L. Wu, R. Jackstell, M. Beller, *Nat. Commun.* **2015**, *6*, 5933-5947; (h) Z. Zhang, T. Ju, J.-H. Ye, D.-G. Yu, *Synlett* **2017**, *28*, 741-750; (i) A. Tortajada, F. Juliá-Hernández, M. Börjesson, T. Moragas, R. Martin, *Angew. Chem. Int. Ed.* **2018**, *57*, 15948-15982; (j) C. S. Yeung, *Angew. Chem. Int. Ed.* **2019**, *58*, 5492; (k) J.-H. Ye, T. Ju, H. Huang, L.-L. Liao, D.-G. Yu, *Acc. Chem. Res.* **2021**, *54*, 2518-2531; (l) J. Davies, J. R. Lyonnet, D. P. Zimin, R. Martin, *Chem* **2021**, *7*, 2927-2942; (m) A. Tortajada, M. Börjesson, R. Martin, *Acc. Chem. Res.* **2021**, *54*, 3941-3952; (n) N. Iwasawa, *Bull. Chem. Soc. Jpn.* **2023**, *96*, 824-841.
- (a) N. Kielland, C. J. Whiteoak, A. W. Kleij, *Adv. Synth. Catal.* **2013**, *355*, 2115-2138; (b) J. Vaitila, Y. Guttormsen, J. K. Mannisto, A. Nova, T. Repo, A. Bayer, K. H. Hopmann, *ACS Catal.* **2017**, *7*, 7231-7244; (c) C.-K. Ran, X.-W. Chen, Y.-Y. Gui, J. Liu, L. Song, K. Ren, D.-G. Yu, *Sci. China Chem.* **2020**, *63*, 1336-1351; (d) X. Guo, Y. Wang, J. Chen., G. Li, J.-B. Xia, *Chin. J. Org. Chem.* **2020**, *40*, 2208-2220.
- For the examples of transition metal catalyzed asymmetric carboxylation with CO₂, see: (a) M. Takimoto, Y. Nakamura, K. Kimura, M. J. Mori, *J. Am. Chem. Soc.* **2004**, *126*, 5956-5957; (b) S. Kawashima, K. Aikawa, K. Mikami, *Eur. J. Org. Chem.* **2016**, *19*, 3166-3170; (c) L. Dian, D.-S. Müller, I. Marek, *Angew. Chem., Int. Ed.* **2017**, *56*, 6783-6787; (d) Y.-Y. Gui, N. Hu, X.-W. Chen, L.-L. Liao, T. Ju, J.-H. Ye, Z. Zhang, J. Li, D.-G. Yu, *J. Am. Chem. Soc.* **2017**, *139*, 17011-17014; (e) X.-W. Chen, L. Zhu, Y.-Y. Gui, K. Jing, Y.-X. Jiang, Z.-Y. Bo, Y. Lan, J. Li, D.-G. Yu, *J. Am. Chem. Soc.* **2019**, *141*, 18825-18835; (f) J. Qiu, S. Gao, C. Li, L. Zhang, Z. Wang, X. Wang, K. Ding, *Chem. Eur. J.* **2019**, *25*, 13874-13878; (g) K.-J. Jiao, Z.-M. Li, X.-T. Xu, L.-P. Zhang, Y. Li, K. Zhang, T.-S. Mei, *Org. Chem. Front.* **2018**, *5*, 2244-2248; (h) X.-W. Chen, J.-P. Yue, K. Wang, Y.-Y. Gui, Y.-N. Niu, J. Liu, C.-K. Ran, W. Kong, W.-J. Zhou, D.-G. Yu, *Angew. Chem. Int. Ed.* **2021**, *60*, 14068-14075; (i) L. Wang, T. Li, S. Perveen, S. Zhang, X. Wang, Y. Ouyang, P. Li, *Angew. Chem. Int. Ed.* **2022**, *61*, e202213943; (j) Y.-Y. Gui, X.-W. Chen, X.-Y. Mo, J.-P. Yue, R. Yuan, Y. Liu, L.-L. Liao, J.-H. Ye, D.-G. Yu, *J. Am. Chem. Soc.* **2024**, *146*, 2919-2927; (k) S. Zhang, L. Li, D. Li, Y.-Y. Zhou, Y. Tang, *J. Am. Chem. Soc.* **2024**, *146*, 2888-2894.
- (a) T. Hoshi, E. Nozawa, M. Katano, T. Suzuki, H. Hagiwara, *Tetrahedron Lett.* **2004**, *45*, 3485-3487; (b) Q. Perron, A. Alexakis, *Adv. Synth. Catal.* **2010**, *352*, 2611-2620; (c) H. Egami, K. Sato, J. Asada, Y. Kawato, Y. Hamashima, *Tetrahedron* **2015**, *71*, 6384-6388.
- For selected examples, see: (a) T. Hashimoto, K. Maruoka, *J. Am. Chem. Soc.* **2007**, *129*, 10054-10055; (b) B. Xu, L. Shi, Y. Zhang, Z. Wu, L. Fu, C. Luo, L. Zhang, Y. Peng, Q. Guo, *Chem. Sci.*, **2014**, *5*, 1988-1991; (c) J. Chen, X. Gong, J. Li, Y. Li, J. Ma, C. Hou, G. Zhao, W. Yuan, B. Zhao, *Science* **2018**, *360*, 1438-1442; (d) L. Lin, S. Fukagawa, D. Sekine, E. Tomita, T. Yoshino, S. Matsunaga, *Angew. Chem. Int. Ed.* **2018**, *57*, 12048-12052; (e) T. Zhou, P. Qian, Y. Li, Y. Zhou, H. Li, H. Chen, B.-F. Shi, *J. Am. Chem. Soc.* **2021**, *143*, 6810-6816; (f) I. Triandafillidi, M. Kokotou, D. Lotter, C. Sparr, C. Kokotos, *Chem. Sci.*, **2021**, *12*, 10191-10196; (g) Q. Wang, Q. Gu, S.-L. You, *Angew. Chem. Int. Ed.* **2019**, *58*, 6818-6825.
- During the manuscript preparation, Yu, Gui, and their co-workers reported a Ni-catalyzed reductive enantioconvergent carboxylation of aza-biaryl triflates with CO₂ using Zn powder as a reductant, X.-W. Chen, C. Li, Y.-Y. Gui, J.-P. Yue, Q. Zhou, L.-L. Liao, J.-W. Yang, J.-H. Ye, D.-G. Yu, *Angew. Chem. Int. Ed.* **2024**, e202403401.

- [11] N. Ishida, Y. Masuda, S. Uemoto, M. A. Murakami, *Chem. Eur. J.* **2016**, *22*, 6524-6527.
- [12] (a) K. Murata, N. Numasawa, K. Shimomaki, J. Takaya, N. Iwasawa, *Chem. Commun.* **2017**, *53*, 3098-3101; (b) K. Murata, N. Numasawa, K. Shimomaki, J. Takaya, N. Iwasawa, *Front. Chem.* **2019**, *7*, 371.
- [13] For the examples under visible light, see: (a) Q.-Y. Meng, S. Wang, B. König, *Angew. Chem. Int. Ed.* **2017**, *56*, 13426-13430; (b) Q.-Y. Meng, S. Wang, G. S. Huff, B. König, *J. Am. Chem. Soc.* **2018**, *140*, 3198-3201; (c) B. Sahoo, P. Bellotti, F. Juliá-Hernández, Q.-Y. Meng, S. Crespi, B. König, R. Martin, *Chem. Eur. J.* **2019**, *25*, 9001-9005; (d) M.-C. Fu, J.-X. Wang, W. Ge, F.-M. Du, Y. Fu, *Org. Chem. Front.* **2023**, *10*, 35-41; (e) J. Davies, J. R. Lyonnet, B. Carvalho, B. Sahoo, C. S. Day, F. Juliá-Hernández, Y. Duan, Á. Velasco-Rubio, M. Obst, P.-O. Norrby, K. H. Hopmann, R. Martin, *J. Am. Chem. Soc.* **2024**, *146*, 1753-1755. For the examples under UV-light, see: (f) N. Ishida, Y. Masuda, Y. Imamura, K. Yamazaki, M. Murakami, *J. Am. Chem. Soc.* **2019**, *141*, 19611-19615; (g) K. Takahashi, Y. Sakurazawa, A. Iwai, N. Iwasawa, *ACS Catal.* **2022**, *12*, 3776-3781.
- [14] (a) K. Shimomaki, K. Murata, R. Martin, N. Iwasawa, *J. Am. Chem. Soc.* **2017**, *139*, 9467-9470; (b) K. Shimomaki, T. Nakajima, J. Caner, N. Toriumi, N. Iwasawa, *Org. Lett.* **2019**, *21*, 4486-4489; (c) S. K. Bhunia, P. Das, S. Nandi, R. Jana, *Org. Lett.* **2019**, *21*, 4632-4637; (d) Y. Jin, N. Toriumi, N. Iwasawa, *ChemSusChem* **2022**, *15*, e202102095.
- [15] J. Hou, A. Ee, W. Feng, J.-H. Xu, Y. Zhao, J. Wu, *J. Am. Chem. Soc.* **2018**, *140*, 5257-5263.
- [16] B. Zhang, T.-T. Li, Z.-C. Mao, M. Jiang, Z. Zhang, K. Zhao, W.-Y. Qu, W.-J. Xiao, J.-R. Chen, *J. Am. Chem. Soc.* **2024**, *146*, 1410-1422.
- [17] (a) A. Ros, B. Estepa, P. Ramírez-López, E. Álvarez, R. Fernández, J. M. Lassaletta, *J. Am. Chem. Soc.* **2013**, *135*, 15730-15733; (b) V. Bhat, S. Wang, B. M. Stoltz, S. C. Virgil, *J. Am. Chem. Soc.* **2013**, *135*, 16829-16832; (c) P. Ramírez-López, A. Ros, A. Romero-Arenas, J. Iglesias-Sigüenza, R. Fernández, J. M. Lassaletta, *J. Am. Chem. Soc.* **2016**, *138*, 12053-12056; (d) J. Carmona, V. Hornillos, P. Ramírez-López, A. Ros, J. Iglesias-Sigüenza, E. Gómez-Bengoa, R. Fernández, J. M. Lassaletta, *J. Am. Chem. Soc.* **2018**, *140*, 11067-11075.
- [18] Using Ni/photoredox catalysis reported in reference [12a], the reductive cross-electrophile coupling between aryl bromide and alkyl bromide occurred to give the alkylated arene as the main by-product.
- [19] N. Toriumi, K. Shimomaki, J. Caner, K. Murata, R. Martin, N. Iwasawa, *Bull. Chem. Soc. Jpn.* **2021**, *94*, 1846-1853.
- [20] P.-P. Zhang, W.-C. Zhang, T.-F. Zhang, Z.-Q. Wang, W.-J. Zhou, *J. Chem. Soc. Chem. Commun.* **1991**, 491-492.
- [21] Y. Lv, B. Wang, H. Yu, *Chin. Chem. Lett.* **2020**, *32*, 1403-1406.



An efficient synergistic photoredox/Pd catalysis was developed to realize the asymmetric cross-electrophile esterification with CO₂, affording a series of axially chiral esters in high yields with excellent enantioselectivities. Key to success was the utilization of an appropriate amount of alkyl bromide to trap the generated chiral carboxylic anion in situ towards the formation of a conformationally stable ester.